Eur. Phys. J. B **51**, 331–336 (2006)
DOI: 10.1140/epjb/e2006-00223-9

THE EUROPEAN PHYSICAL JOURNAL B

Enumeration of many-body skeleton diagrams

L.G. Molinari[1,2] and N. Manini[1,3,a]

[1] Dipartimento di Fisica dell'Università degli Studi di Milano, via Celoria 16, 20133 Milano, Italy
and
European Theoretical Spectroscopy Facility (E.T.S.F.), Milan node, Italy
[2] I.N.F.N. Sezione di Milano, Italy
[3] INFM - CNR, Unità di Milano, Milano, Italy

Received 24 February 2006
Published online 13 June 2006 –

Abstract. The many-body dynamics of interacting electrons in condensed matter and quantum chemistry is often studied at the quasiparticle level, where the perturbative diagrammatic series is partially resummed. Based on Hedin's equations for self-energy, polarization, propagator, effective potential, and vertex function, dressed (skeleton) Feynman diagrams are enumerated. Such diagram counts provide useful simple checks for extensions of the theory for future realistic simulations.

PACS. 71.10.-w Theories and models of many-electron systems – 24.10.Cn Many-body theory – 11.10.Gh Renormalization

1 Introduction

Current research in electronic properties of molecules, nanocomponents, and solids has gone far beyond the mean-field density-functional description. Many-body methods are employed routinely, at the level of quasiparticles, to describe excitations accurately [1–3]. Propagators and interactions are renormalized to obtain an effective theory of weakly interacting quasiparticles. This is achieved by infinite resummations of Feynman diagrams, that are brought to a smaller class of skeleton diagrams [4]. The reduction in number should correspond to better analytic behavior in space-time of the individual dressed diagrams, as it occurs in random-phase or ladder resummations [5].

In this report, we extend the method proposed in reference [6] to the enumeration of skeleton Feynman diagrams within several renormalization schemes for the exact many-body theory and its GW approximation [1–3]. Enumeration of Feynman diagrams is useful in various contexts: as a check for any diagrammatic approach to the many-body problem in realistic dimensions, for graph and knot theory, and in statistical mechanics. For example, diagram counting allowed to establish the exact solution of a model of 1D electrons in a random potential [7,8]; this solution exhibits non-Fermi-liquid properties that are encountered in models for high-T_c superconductivity [9,10]. The study of band random matrices is relevant for quantum chaos and the theory of transport in presence of disorder: spectral density correlators were evaluated by counting planar Feynman diagrams [11]. In statistical mechanics, the enumeration of planar Feynman diagrams of matrix models [12] was used for the enumeration of configurations in models of two-dimensional random lattices [13], in the classification of knots [14], in the four-colour problem [15]. Finally, the asymptotics of diagram enumeration is important to estimate convergence properties of renormalized expansions of field-theoretical models [16–18].

We take as our starting point the standard formulation of the many-body problem of N interacting fermions provided by the set of five Hedin's equations [2,3,19,20] for the propagator $G(1,2)$, effective potential $W(1,2)$, irreducible self-energy $\Sigma(1,2)$, irreducible polarization $\Pi(1,2)$, and irreducible vertex $\Gamma(1;2,3)$, where 1 is a shorthand notation for a full space-time coordinate $(\boldsymbol{x}_1, t_1)$.

$$G(1,2) = g(1,2) + g(1,1')\,\Sigma(1',2')\,G(2',2) \tag{1}$$

$$W(1,2) = v(1,2) + v(1,1')\,\Pi(1',2')\,W(2',2) \tag{2}$$

$$\Sigma(1,2) = i\Gamma(2';1,1')\,G(1',2)\,W(2',2) \tag{3}$$

$$\Pi(1,2) = -2i\Gamma(1;2',1')\,G(2,2')\,G(1',2) \tag{4}$$

$$\Gamma(1;2,3) = \delta(1,2)\,\delta(1,3) + \Gamma(1;2',3')\,G(1',2')\,G(3',4')\,\frac{\delta\Sigma(2,3)}{\delta G(1',4')}. \tag{5}$$

Repeated primed space-time variables are understood to be integrated. $g(1,2)$ is the Green function of the interacting system in the Hartree approximation, with exact particle density, so that Hartree-type insertion (tadpoles) are

[a] e-mail: nicola.manini@mi.infm.it

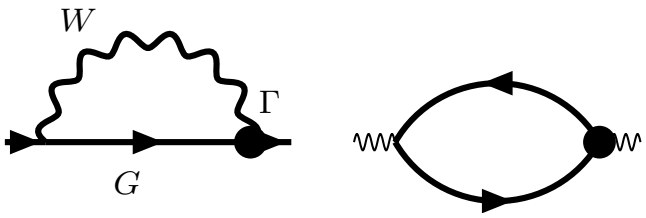

Fig. 1. The unique fully dressed skeleton diagrams for self-energy (left) and polarization (right).

already accounted for. The five exact Hedin's equations are formally closed, at the price of a functional derivative. A different functional closure of Schwinger-Dyson equations, leading to diagrammatic recursion schemes, was developed by Pelster et al. [21,22].

The diagrammatic meaning of Hedin's equations is simple: equations (1, 2) correspond to Dyson's equations that define the proper self-energy and polarization insertions for the propagator and the effective potential, equations (3, 4) translate the unique skeleton structure [5] of Σ and Π, shown in Figure 1. Finally, the vertex equation (5) shows that vertex diagrams arise from self-energy diagrams, by "pinching" a G line with a vertex (remove a line G and replace it with $G\Gamma G$): this follows from the functional definition of the vertex [6,19,23]. The tremendous difficulty of the vertex equation is avoided in the GW approximation, where vertex corrections are neglected and the bare vertex is used in the other equations. The four integral GW equations that result, are closed and are being currently used in many-body calculations. The challenge of including vertex corrections is still open [1,24,25]. In the present work we take advantage of the simplifications characteristic of zero space-time dimensions to solve exactly the complete set (1–5).

2 Enumeration of Feynman diagrams

In zero dimension of space *and* time, the combinatorial content of Wick's expansion survives, producing the same Feynman diagrams in the perturbative expansion of the correlators as in conventional 3+1 dimensions. The correlators no longer carry space-time labels, and do not correspond to space-time functions. However, they continue to solve Hedin's equations, which can indeed be derived from considerations about the topology of diagrams [4]. Four of Hedin's equations become algebraic, in terms of the scalar variables g and v, representing the Hartree propagator and the bare interparticle interaction respectively. The functional derivative in the equation for the vertex becomes an ordinary derivative. The five equations read:

$$G = g + g\Sigma G, \qquad W = v + v\Pi W, \tag{6}$$

$$\Sigma = iGW\Gamma, \qquad \Pi = i\ell G^2\Gamma, \tag{7}$$

$$\Gamma = 1 + \Gamma G^2 \tfrac{\partial\Sigma}{\partial G}. \tag{8}$$

A useful parameter ℓ is here introduced to count fermion loops, and replaces the value -2 in Hedin's equation (4). In the GW approximation all corrections to the bare vertex are neglected: the approximation $\Gamma = 1$ replaces the exact vertex equation (8).

The perturbative solution of Hedin's equations in zero dimension provides numerical coefficients which enumerate the Feynman diagrams for the five correlators involved. The ordinary perturbation expansion is carried out in the bare parameters v and g. However, it is often convenient to expand in different "renormalized" variables, such as v and G, or W and G, or G,W and Γ. These expansions count Feynman diagrams where, respectively, the propagator or both the propagator and the potential, or also the vertex, have been fully renormalized. Such diagrams where self-energy contributions of various types are resummed, are called *skeleton* graphs [4,5]. In this paper we extend the method of enumeration of bare diagrams developed in reference [6] to the problem of counting skeleton diagrams. Different levels of resummations will be considered below, including a renormalization based on GW correlators.

2.1 $x = g^2v$-expansion

The standard perturbation theory in the bare interaction v has been studied in $d = 0$ by various authors, either by a combinatorial analysis [26], or by the path-integral formulation of the interacting field, which degenerates to an ordinary integral [27–29]. An approach based on Hedin's equations is very convenient to deal with the Hartree propagator g in place of the bare one, and explicit counting numbers were obtained [6]. It is useful to rederive here the main equations for the propagator and the vertex.

Here, the natural dimensionless expansion parameter is $x = ig^2v$. We provide the equation for $Z(x) = G/g$, where Z is the renormalization factor due to self-energy corrections. The algebraic equations (6, 7) yield

$$\ell x Z^2(x)\Gamma(x) = 1 - \frac{1}{1 - \ell + \ell Z(x)}. \tag{9}$$

The GW approximation ($\Gamma = 1$), generates a cubic equation for Z_{GW}. For the complete theory, we rewrite the vertex equation (8), in a form [6] where G is traded for g:

$$\Gamma(x) = 1 + g^2\frac{\partial\Sigma}{\partial g} = \frac{1}{Z(x)} - 2x\frac{d}{dx}\frac{1}{Z(x)}. \tag{10}$$

Equations (9) and (10) combine to a closed equation for Z:

$$2\ell x^2\frac{dZ}{dx} = 1 - \ell x Z(x) - \frac{1}{1 - \ell + \ell Z(x)}, \tag{11}$$

with the initial condition $Z(0) = 1$. The solution as a series expansion in x provides the number of Feynman diagrams that contribute to each order to the propagator G

$$Z(x) = 1 + x + (3 + \ell)x^2 + (15 + 11\ell + \ell^2)x^3 + \dots \tag{12}$$

The ℓ powers represent the loop contents. For example, at second order in x, the theory involves 3 diagrams with no loops, and 1 diagram with one loop; they are shown

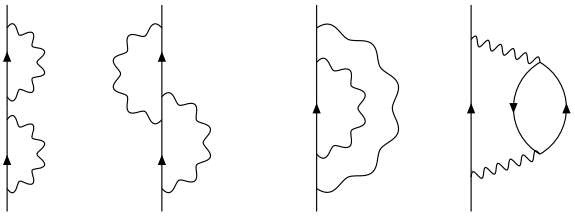

Fig. 2. The four diagrams for G at second order in x.

in Figure 2. Higher-order diagrams are drawn in reference [30]. By substituting the power series for $Z(x)$ into equation (10), we obtain the diagram count for the vertex function:

$$\Gamma(x) = 1+x+3\,(2+\ell)\,x^2+5\left(10+9\,\ell+\ell^2\right)x^3+\ldots \quad (13)$$

Table 1 reports the total number of vertex diagrams up to 10th order, obtained by taking $\ell = 1$ in the expansion for $\Gamma(x)$.

2.2 y = G²v-skeleton expansion

When all self-energy insertions of the propagator are resummed, one ends up with Feynman diagrams where the propagator lines correspond to the exact G, while the interaction lines continue to correspond to the bare v. This resummation is obtained by using the expansion parameter $y = iG^2v$. It is possible to obtain a closed equation for the vertex function. First write the self-energy as

$$\Sigma = iGW\Gamma = iG\frac{v}{1-v\Pi}\Gamma = \frac{1}{G}\frac{y\Gamma}{1-y\ell\Gamma}. \quad (14)$$

Next evaluate the vertex function in equation (8) by means of equation (14), and obtain a differential equation for $\Gamma(y)$:

$$2y^2\Gamma\frac{d\Gamma}{dy} = -1+(1+2y\ell)\Gamma - y\Gamma^2(1+2\ell+y\ell^2) + y^2\Gamma^3\ell(\ell-1). \quad (15)$$

This equation must be solved with the initial condition $\Gamma(0) = 1$. The series expansion of the solution counts skeleton vertex diagrams with dressed propagators and bare interactions:

$$\Gamma(y) = 1+y+(4+3\ell)y^2+(27+31\ell+5\ell^2)y^3+\ldots \quad (16)$$

Table 1 lists the total number of these diagrams up to order $n = 10$, by taking $\ell = 1$ in the expansion for $\Gamma(y)$, as was done above.

The enumeration of skeleton diagrams of the polarization $\Pi = i\ell G^2\Gamma(y)$ coincides with that of $\Gamma(y)$. The skeleton expansion of Σ results from equation (14):

$$\Sigma/iGv = 1+(1+\ell)y+(4+5\ell+\ell^2)y^2 + (27+40\ell+14\ell^2+\ell^3)y^3+\ldots \quad (17)$$

In the ordinary perturbative (x) expansion, Π and Σ share the diagram counting [6]. In contrast, this property is lost in the y expansion at hand.

The removal of loops from G^2v enumerations is obtained by setting $\ell = 0$, and selects diagrams with dressed propagators and intersecting potential arches. These diagrams arise in the evaluation of the average self energy for a single particle in a white-noise external field [31]. Indeed equation (15) with $\ell = 0$ coincides with equation (18) of reference [31]. The asymptotic enumeration of such graphs was also considered by Suslov [32], in the study of Anderson's localization of a particle in a random potential.

The G^2v-expansion of Σ is interesting for the theory of the Luttinger-Ward Φ-functional [33,34]. By closing all $\Sigma[G,v]$ skeleton graphs with a G line, and dividing each one by the number of G lines it contains, one obtains a functional with the property of yielding the self-energy and the reducible polarization:

$$\Sigma(1,2) = \frac{\delta\Phi[G,v]}{\delta G(2,1)}, \qquad \tilde{\Pi}(1,2) = -2\frac{\delta\Phi[G,v]}{\delta v(2,1)}. \quad (18)$$

In $d = 0$, the functional $\Phi[G,v]$ turns into an ordinary function of $y = iG^2v$:

$$\Phi(y) = \frac{1}{2}\int_0^y dy'\frac{\Gamma(y')}{1-\ell y'\Gamma(y')} = \frac{y}{2}+(1+\ell)\frac{y^2}{4}+(4+4\ell+\ell^2)\frac{y^3}{6}+\ldots \quad (19)$$

This last expression provides the appropriate diagram counting and fractional weights for $\Phi(y)$ in any dimension.

2.3 z = G²W-skeleton expansion

Resummation of both self-energy and polarization insertions leads to skeleton diagrams with exact propagators G and interactions W. Here, the natural expansion parameter is $z = iG^2W$. The parameter z is linked as follows

$$z = iG^2\frac{v}{1-i\ell v\Gamma G^2} = \frac{y}{1-\ell y\Gamma} \quad (20)$$

to the parameter $y = iG^2v$ of the previous section. Inversion yields $y = z\,[1+\ell z\Gamma(z)]^{-1}$. By entering this relation into the differential equation (15) for $\Gamma(y)$, which is now viewed as a function of z, we obtain

$$z^2\frac{d\Gamma(z)}{dz} = \frac{1-\Gamma(z)+z\Gamma^2(z)+2\ell z^2\Gamma^3(z)}{\ell-(2+\ell)\Gamma(z)-3z\ell\Gamma^2(z)}. \quad (21)$$

The appropriate series expansion counts G^2W-dressed vertex diagrams:

$$\Gamma(z) = 1+z+2\,(2+\ell)\,z^2+(27+22\ell)\,z^3+\ldots \quad (22)$$

Table 1 lists the total number of these $\Gamma(z)$ diagrams up to order $n = 10$. Both $\Sigma = iGW\Gamma(z)$ and $\Pi = i\ell G^2\Gamma(z)$ have the same total G^2W-counting numbers as the vertex.

Table 1. The number of nth-order skeleton diagrams for the vertex function in the five renormalization schemes considered in the text.

n	1	2	3	4	5	6	7	8	9	10
$\Gamma(x)$	1	9	100	1323	20 088	342 430	6 461 208	133 618 275	3 006 094 768	73 139 285 178
$\Gamma(y)$	1	7	63	729	10 113	161 935	2 923 135	58 547 761	1 286 468 225	30 747 331 223
$\Gamma(t)$	1	6	52	602	8223	128 917	2 273 716	44 509 914	957 408 649	22 449 011 336
$\Gamma(z)$	1	6	49	542	7278	113 824	2 017 881	39 842 934	865 391 422	20 486 717 908
$\Gamma(u)$	1	3	13	147	1965	30 979	559 357	11 289 219	250 794 109	6 066 778 627

In the G^2W-expansion, it is natural to define [33,35] the functional $\Psi[G,W]$, which generalizes equation (18) and generates the self-energy and the irreducible polarization as follows:

$$\Sigma(1,2) = \frac{\delta\Psi[G,W]}{\delta G(2,1)}, \qquad \Pi(1,2) = -2\frac{\delta\Psi[G,W]}{\delta W(2,1)}. \quad (23)$$

The diagrammatic construction of Ψ is the same as for Φ: close the skeleton graphs of $\Sigma = iGW\Gamma[G,W]$ with a G line and divide by the number of G lines that the graph contains. In $d = 0$ we have $G\Sigma = z\Gamma(z)$; to divide by the number of G lines that each $G\Sigma$-diagram contains, corresponds to the integral

$$\Psi(z) = \frac{1}{2}\int_0^z dz'\Gamma(z') = \frac{z}{2} + \frac{z^2}{4} + (2+\ell)\frac{z^3}{3} + \dots \quad (24)$$

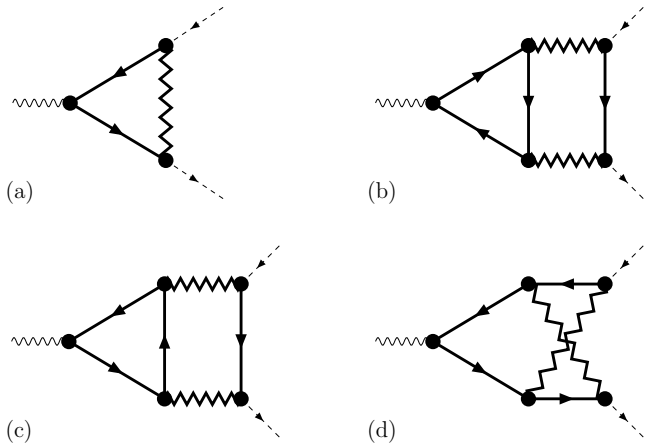

Fig. 3. All first-order (a) and second-order (b, c, d) vertex diagrams in u expansion.

2.4 u = $G^2W\Gamma^2$-skeleton expansion

The G^2W-expansion resums all self-energy and polarization insertions, and skeleton diagrams of various order in z result just because of vertex contributions. If vertex diagrams are summed as well, each of the self-energy and the polarization is brought to a unique skeleton diagram depicted in Figure 1. Vertex diagrams cannot be brought to a finite collection of skeleton diagrams. We may nevertheless resum vertex insertions in all vertex diagrams, and enumerate the resulting vertex skeleton diagrams, where all lines and vertices are resummed.

This is achieved by noting that in a vertex diagram, each W line ends in two vertices. However, the vertex which the interaction external line is attached to, is left out (see Fig. 3 for some vertex diagrams). We then write $\Gamma = 1 + \Gamma\gamma(u)$, in terms of the expansion variable $u = iG^2W\Gamma^2 = z\Gamma^2(z)$. The factor Γ in front of $\gamma(u)$ accounts for the left-out vertex.

The Taylor expansion of $\gamma(u)$ enumerates all dressed fully renormalized vertex diagrams. An equation for γ is obtained from the relation

$$\frac{d\gamma}{du} = \frac{dz}{du}\frac{d}{dz}\frac{\Gamma-1}{\Gamma} = \frac{1}{\Gamma^2}\frac{d\Gamma/dz}{\Gamma^2 + 2z\Gamma d\Gamma/dz}, \quad (25)$$

where we enter $d\Gamma/dz$ given by equation (21):

$$u\frac{d\gamma}{du} = (1-\gamma)\frac{2\ell u^2(1-\gamma)^2 + u(1-\gamma) - \gamma}{\ell u^2(1-\gamma)^2 - \ell u\gamma(1-\gamma) - 2\gamma}. \quad (26)$$

This equation is solved with initial condition $\gamma(0) = 0$. The resulting u-expansion for Γ is

$$\Gamma(u) = 1 + (\Gamma u) + (1+2\ell)(\Gamma u^2) + (7+6\ell)(\Gamma u^3) + (63 + 74\ell + 10\ell^2)(\Gamma u^4) + \dots \quad (27)$$

The diagrams of first and second order are shown in Figure 3 (the next 13 third-order diagrams coincide with those of QED, drawn in Ref. [28]). This u-expansion represents the "ultimate" skeleton expansion, where all ingredients of Hedin's equations have been renormalized. Indeed, as apparent in Table 1, the diagram count is smallest in the u expansion at hand.

2.5 t = $(G^2W)_{GW}$-skeleton expansion

In the GW approximation ($\Gamma = 1$), in physical dimensions, Hedin's equations are a system of ordinary integral equations for G_{GW}, Σ_{GW}, W_{GW} and Π_{GW}. It is conceivable that in a near future increased computer power will allow us to solve these equations in fully self-consistent GW: this would make the GW approximation the zeroth-order stage of a subsequent attack of the full many-body problem, where vertex corrections are included perturbatively. The problem of including vertex corrections in a systematic way is an important target of present-day research, to overcome several limitations of the non-conservative GW [1,24,25]. It is therefore of interest to count the diagrams where g and v lines are dressed (resummed) to include all their GW self-energy and polarization insertions.

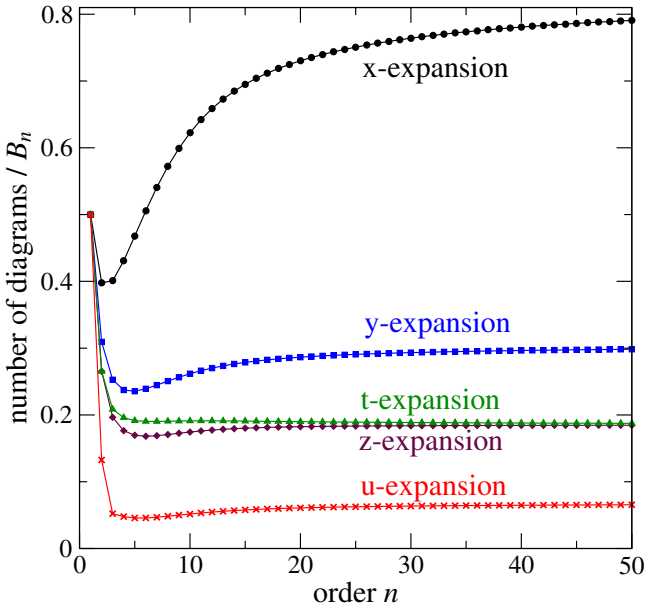

Fig. 4. (Color online) Number of vertex diagrams at order n, divided by the asymptotic expression B_n defined in equation (32), for the different renormalization schemes realized in Section 2.1 [x – Eq. (12)], Section 2.2 [y – Eq. (16)], Section 2.5 [t – Eq. (31)], Section 2.3 [z – Eq. (22)], and Section 2.4 [u – Eq. (27)].

The counting problem is solved in $d = 0$ by considering the expansion parameter $t = iG_{GW}^2 W_{GW}$. With simple algebra, the following two equations for the vertex and the ratio $Z_{GW}(t) = G/G_{GW}$ are obtained:

$$tZ_{GW}^2(t)\Gamma(t) = \frac{[(1+t)Z_{GW}(t)-1](1+\ell t)}{1-\ell+\ell(1+t)Z_{GW}(t)}, \tag{28}$$

$$2t^2\frac{dZ_{GW}}{dt} = (1-t-2\ell t^2)\frac{(1+t)Z_{GW}(t)-1}{1-\ell+\ell(1+t)Z_{GW}(t)} - \frac{t}{1+\ell t}Z_{GW}(t). \tag{29}$$

The perturbative solutions are:

$$Z_{GW}(t) = 1 + t^2 + (5+3\ell)t^3 + \ldots \tag{30}$$

$$\Gamma(t) = 1 + t + 2(2+\ell)t^2 + (29+23\ell)t^3 + \ldots \tag{31}$$

Table 1 lists the total number of these $\Gamma(t)$ diagrams up to order $n = 10$.

3 Asymptotics

To estimate asymptotic behaviors is not simple in the present approach. However, the topology of many-body diagrams with two-body interaction is the same as in relativistic quantum electrodynamics (QED), with a difference: because of exact particle-antiparticle symmetry, QED diagrams with loops involving an odd number of fermion lines cancel (Furry's theorem [23]). Therefore, many-body skeleton diagrams grow faster in number than QED ones.

The functional approach, in the saddle point expansion, is better suited for asymptotics. This problem in physical dimensions has been studied for QED by several authors, based on Lipatov's powerful method [36,16]. From the tabulated QED asymptotic values [28] in $d = 0$, one can infer the leading behavior of many-body vertex skeleton diagrams. Consider the series for the vertex $\Gamma(\theta) = \sum_n A_n\theta^n$, in one of the renormalization schemes ($\theta = x,\ y,\ z,\ t,\ u$) outlined above. We obtain

$$A_n = B_n\,(c_0 + c_1/n + \ldots), \qquad B_n = n!\,2^n\,n^{3/2}. \tag{32}$$

In Figure 4 the asymptotic behavior is checked on the first 50 coefficients of the five different vertex skeleton expansions computed in the present work. Indeed, in all expansions, whether bare or renormalized, the number of vertex diagrams grows with the order n roughly as B_n, thus leading to divergent power series, like in QED. The renormalization scheme only affects the subleading coefficients c_i. As expected, the "ultimate" u expansion, involving wider diagram resummations leads to fewer diagrams than all other "less renormalized" expansions. For large n, the diagram count is essentially the same for the z expansion, including renormalization to both the propagator and the interaction, and for the t expansion around Hedin's GW approximation.

4 Conclusions

The present method for enumerating skeleton diagrams is based on Hedin's equations and it is very efficient. We obtain different renormalization schemes by simple changes of the expansion variable in differential equations that can be solved by series. The coefficients of these series are integers that count skeleton diagrams. As expected, the number of diagrams, whether renormalized or not, grows factorially with the order.

This work was funded in part by the EU's 6th Framework Programme through the NANOQUANTA Network of Excellence (NMP4-CT-2004-500198).

References

1. G. Onida, L. Reining, A. Rubio, Rev. Mod. Phys. **74**, 601 (2002)
2. W.G. Aulbur, L. Jönsson, J.W. Wilkins, Solid State Physics, edited by H. Ehrenreich, F. Spaepen (Academic, New York, 2000), Vol. 54, p. 1
3. F. Aryasetiawan, O. Gunnarsson, Rep. Progr. Phys. **61**, 237 (1998)
4. J.D. Bjorken, S.D. Drell, *Relativistic Quantum Fields* (McGraw Hill, New York, 1965)
5. A.L. Fetter, J.D. Walecka, *Quantum Theory of Many-Particle Systems* (McGraw-Hill, New York, 1971)
6. L.G. Molinari, Phys. Rev. B **71**, 113102 (2005)

7. M.V. Sadovskiĭ, Soviet Physics JETP **50**, 989 (1979)
8. M.V. Sadovskiĭ, A.A. Timofeev, J. Moscow Phys. Soc. **1**, 391 (1991)
9. R.H. McKenzie, D. Scarratt, Phys. Rev. B **54**, R12709 (1996)
10. J. Schmalian, D. Pines, B. Stojković, Phys. Rev. B **60**, 667 (1999)
11. J. D'Anna, A. Zee, Phys. Rev. E **53**, 1399 (1996)
12. E. Brézin, C. Itzykson, G. Parisi, J.B. Zuber, Comm. Math. Phys. **59**, 35 (1978)
13. D.V. Boulatov, V.A. Kazakov, Phys. Lett. B **186**, 379 (1987)
14. P. Zinn-Justin, *Some Matrix Integrals related to Knots and Links*, in *Random Matrix Models and their Applications*, MSRI Publications, Vol. 40, edited by P. Bleher, A. Its (Cambridge University Press, 2001) e-print `arXiv:math-ph/9910010`
15. G. Cicuta, L. Molinari, E. Montaldi, Phys. Lett. B **306**, 245 (1993)
16. I.M. Suslov, Zh. Eksp. Teor. Fiz. **127**, 1350 (2005); I.M. Suslov, Sov. Phys. JETP **100**, 1188 (2005) e-print `arXiv:hep-th/0510142`
17. G. Parisi, Phys. Lett. B **68**, 361 (1977)
18. B. Lautrup, Phys. Lett. B **69**, 109 (1977)
19. L. Hedin, Phys. Rev. **139**, A796 (1965)
20. L. Hedin, S. Lundqvist, *Solid State Physics*, edited by F. Seitz, D. Turnbull, H. Ehrenreich (Academic, New York, 1969), Vol. 23, p. 1
21. A. Pelster, H. Kleinert, M. Bachmann, Ann. Phys. **297**, 363 (2002)
22. A. Pelster, K. Glaum, Phys. Status Solidi B **237**, 72 (2003)
23. C. Itzykson, J.P. Zuber, *Quantum Field Theory* (McGraw Hill, New York, 1980)
24. A. Schindlmayr, R.W. Godby, Phys. Rev. Lett. **80**, 1702 (1998)
25. F. Bruneval, F. Sottile, V. Olevano, R. Del Sole, L. Reining, Phys. Rev. Lett. **94**, 186402 (2005)
26. R.J. Riddell, Phys. Rev. **91**, 1243 (1953)
27. A.G. Basuev, A.N. Vasil'ev, Theor. Math. Phys. **18**, 129 (1974)
28. P. Cvitanovic, B. Lautrup, R.B. Pearson, Phys. Rev. D **18**, 1939 (1978)
29. E.N. Argyres, A.F.W. van Hameren, R.H.P. Kleiss, C.G. Papadopoulos, Eur. Phys. J. C **19**, 567 (2001)
30. R.J. Mathar, e-print `arXiv:physics/0512022`
31. É.Z. Kuchinskiĭ, M.V. Sadovskiĭ, J. Exp. Theor. Phys. **86**, 367 (1998)
32. I.M. Suslov, Sov. Phys. JETP **75**, 1049 (1992)
33. C.-O. Almbladh, U. Von Barth, R. Van Leeuwen, Int. J. Mod. Phys. B **13**, 535 (1999)
34. G.F. Giuliani, G. Vignale, *Quantum Theory of the Electron Liquid* (Cambridge University Press, 2005)
35. K. Kajantie, M. Laine, Y. Schröder, Phys. Rev. D **65**, 045008 (2002)
36. C. Itzykson, G. Parisi, J.B. Zuber, Phys. Rev. D **16**, 996 (1977)